

Review

Unravelling the Environmental Application of Biochar as Low-Cost Biosorbent: A Review

Antía Fdez-Sanromán, Marta Pazos , Emilio Rosales *  and María Angeles Sanromán 

CINTECX, Universidade de Vigo, Department of Chemical Engineering, Campus Universitario as Lagoas—Marcosende, E-36310 Vigo, Spain; antia.fernandez@alumnos.uvigo.es (A.F.-S.); mcurras@uvigo.es (M.P.); sanroman@uvigo.es (M.A.S.)

* Correspondence: emilirov@uvigo.es; Tel.: +34-986-812-383

Received: 9 October 2020; Accepted: 2 November 2020; Published: 4 November 2020



Abstract: In this age, a key target for enhancing the competitiveness of the chemical, environmental and biotechnology industries is to manufacture high-value products more efficiently and especially with significantly reduced environmental impact. Under this premise, the conversion of biomass waste to a high-value added product, biochar, is an interesting approach under the circular economy principles. Thus, the improvements in the biochar production and its new and innovative uses are hot points of interest, which are the focus of vast efforts of the scientific community. Biochar has been recognized as a material of great potential, and its use as an adsorbent is becoming a reliable strategy for the removal of pollutants of different streams, according to its high adsorption capacity and potential to eliminate recalcitrant compounds. In this review, a succinct overview of current actions developed to improve the adsorption capability of biochar, mainly of heavy metal and organic pollutants (dyes, pharmaceuticals and personal care products), is summarized and discussed, and the principal adsorption mechanisms are described. The feedstock and the production procedure are revealed as key factors that provide the appropriate physicochemical characteristics for the good performance of biochar as an adsorbent. In addition, the modification of the biochar by the different described approaches proved their feasibility and became a good strategy for the design of selective adsorbents. In the last part of this review, the novel prospects in the regeneration of the biochar are presented in order to achieve a clean technology for alleviating the water pollution challenge.

Keywords: adsorption; biochar; micropollutants; heavy metals; biomass; water pollution

1. Introduction

Nowadays, the environmental crisis and vulnerabilities have attracted the attention of researchers to the hunt for new green and friendly strategies for increasing resources [1]. In addition, the current linear economic system stands out diametrically from the life cycle of nature, in which there is no garbage or landfills are reused for other different stages. In this context, in recent years, the replacement of conventional sources with recoverable wastes has set the pace for the achievement of genuinely revolutionary processes from an environmental perspective [2]. The utilization of these wastes as a raw material has been proposed as one of their principal alternatives, and a brightening industrial future has been recently suggested for them, based on the concept of the circular economy. An example of the circular economy is the transformation of wastes into biochar, which, although initially prepared from non-residual biomass, in recent years have been produced from a wide variety of organic raw materials. Their availability is subject to sustainability requirements, such as not competing with the human food chain or animal and plant nutrition, and coming from a sustainable source for the environment and climate protection [3]. Thus, biochar preparation itself is a process of recycling

organic waste with multiple benefits: waste treatment, environmental protection, and reduction in the biochar processing cost.

Biochar is a carbon-rich product obtained under reducing thermal conditions by the decomposition of organic matter with a limited supply of oxygen [4]. It is comprised of particles with different sizes and has high porosity with micro-, meso-, and macropores, whose sizes range from <2 nm to 2–50 nm and >50 nm, respectively. The macropores come from the spaces of the original raw material, and micropores and mesopores are generated in the thermochemical process [5]. In the production of biochar, researchers have applied several thermochemical methods using several feedstocks, with diverse contents of cellulose, hemicellulose and lignin, leading to different physicochemical properties of biochar [6,7]. As it was explained by Xiao et al. [8], the characterization of the biochar surface could explain its main properties, which are composites of aliphatic and aromatic groups and having abundant functional groups such as hydroxyl, epoxy, carboxyl, carbonyl, ether, ester, amide, sulfonic, and acyl groups as well as minerals and trace metals. Therefore, it is deemed a material that possesses the capacity to exchange electrons and high reactivity.

The potential applications of biochar include as an energy source (biofuel), soil conditioner, and adsorbent [9]. For the last 20 years, the reviewing of the database Scopus[®], by evaluation of articles, reviews and books containing the keyword “biochar”, draws a growing trend in the number of articles published per year, from 1 in 2000 to 3030 in 2019, and over 2341 by July 2020 (Figure 1). Concerning the different applications, the evolution of publications is similar and has increased over the 10 years. As can be seen in Figure 1, most of the articles published are related to the use of biochar as a soil conditioner. This tendency is observed from the beginning, followed by articles related to biofuel. However, from 2006 onwards, this pattern changes, and there is a growing interest in studies related to its usage in the remediation of polluted streams. Currently, the number of papers published so far in 2020 on this subject (1187) is higher than its application as a soil conditioner, which represents around 42% of the papers published in relation to biochar. The adsorption process is currently one of the main technologies applied in wastewater remediation. This fact is corroborated by the analysis of recent studies; thus, the search on the database Scopus[®] of the keywords “biochar” and “adsorption” reveals the exponential growth of the articles published, from 10 in 2009 to nearly 1000 in 2019.

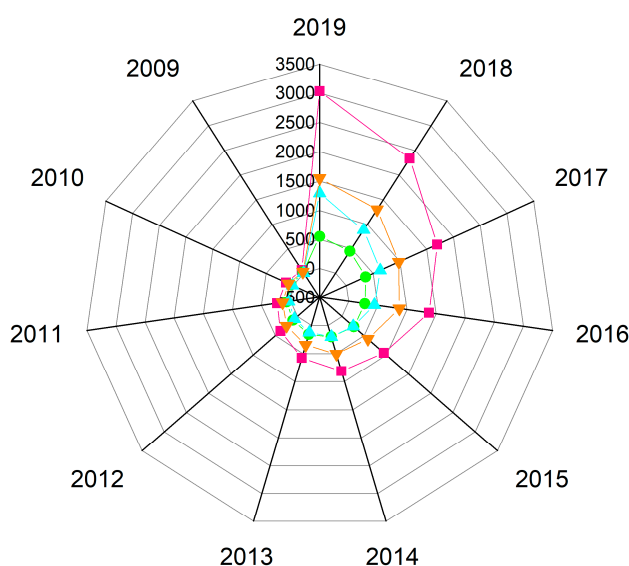


Figure 1. Evolution of papers published in the last decade: pink, total; orange, soil; green, biofuel; and blue, adsorbent (Source: Scopus[®] database).

The particular properties and morphology of biochar make it possible to use it as a suitable sorbent. In addition, this carbon-rich product requires less expensive technology, and its production

demands lower energy requirements compared to more commonly employed adsorbents such as activated carbon [10].

There are diverse production methods, mainly considering thermochemical technologies to transform biomass into biochar. These can be classified into several categories (Figure 2): (i) slow or fast pyrolysis in the complete absence of oxygen, (ii) gasification, which occurs with reduced oxygen atmosphere, (iii) hydrothermal carbonization, applying heating to biomass in the water at subcritical with high levels of oxygen, (iv) dry and wet torrefaction under inert nitrogen and (v) microwave-assisted pyrolysis [11]. The physical and chemical transformations that occur in the fabrication process are very complex and rely on both the nature of the biomass and the conditions of the reactor. These conditions and the characteristics of the raw material (composition, particle size distribution and pore size, among others) largely determine these mentioned properties of the biochar [12]. Furthermore, chemical or physical post-treatments can be applied to the biochar with the aim to enhance surface characteristics or increase its catalytic activity (Figure 2).

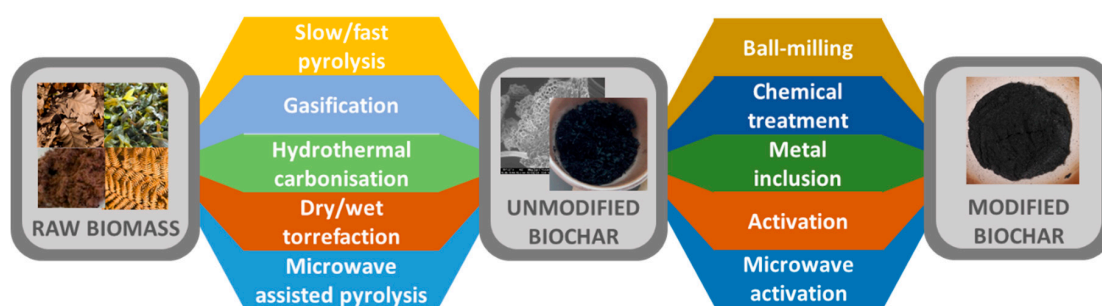


Figure 2. Biochar production methods.

Therefore, based on the increasing interest in its use as an adsorbent, the aim of this review will focus on analyzing the most recent studies on the effect of main production variables in the biochar, discussing their influence in the application to wastewater remediation and evaluating the different strategies employed in order to enhance the uptake capacity of this low-cost adsorbents. An insight into the adsorption mechanism for organic and inorganic contaminants is provided. Furthermore, the recent advances in the regeneration of these carbonaceous adsorbents and the limitations in their use will be also displayed and discussed. Finally, an economic analysis is performed, and future prospects are analyzed.

2. Adsorption Process

The elimination of organic and inorganic pollutants from the aquatic ecosystem is essential due to the increase in the global population, estimated to reach around 9.3 billion by 2050 [13]. Among the different techniques that are being applied today for the rapid removal of organic and inorganic pollutants from wastewater, the adsorption process has increasingly gained attention as a valuable promissory technique. Adsorption is a well-known process, especially in the removal of pollutants from effluents containing moderate or low concentrations pollutants.

Several materials can be used as adsorbents, and their proper selection is largely related to their feasible environmental applications. To consider a material as an ideal adsorbent, it is required to have many characteristics, such as cost-effectiveness, abundance, physical and chemical resistance, morphology and surface chemistry, high specific surface area, user-friendliness or being easily renewable [14]. Other important parameters are its hydrophobic-hydrophilic properties and the functional groups present in the adsorbent [15]. In recent studies, different strategies, such as the loading of metals, oxides or ions, physical and chemical modification and so forth, have been assessed in order to achieve higher adsorption capacity of the existing adsorbents by improving the above-mentioned properties [16].

Numerous studies have demonstrated the applicability of biochar as a low-cost adsorbent, [17,18], a fact confirmed by Yoder et al. [19] who estimated the cost for the production of biochar from feedstock as lower than 0.08 USD/kg, which is lower than 10% of the price of the commercial adsorbents. Generally, biochar is characterized by low apparent density (0.30 to 0.45 g/cm³), high surface area (200–400 m²/g) and high porosity (micro-, meso- and macropores) [20]. Several variables can be selected to ameliorate the biochar properties [21]. In general, as the temperature of the process increases, a greater percentage of gases is produced and the percentage of the solid fraction is reduced, with a similar effect on the surface functional groups of the biochar (C=O and C–H), which is also reduced [22]. Thus, it is necessary to understand better how to act on the different process variables in order to provide the adequate properties to the engineered biochar based on the characteristics of the effluent to treat and the operational scale request.

3. Biochar Adsorption of Heavy Metals

It is known that some heavy metals are essential to organisms in small amounts, such as Fe, Mn, Zn, B, V, Cu, Ni or Mo, but become harmful when they are present in high concentrations, while others, such as Cd, Cr, Hg or Pb, have no biological function and are highly toxic. Currently, mining operations, metal plating facilities, industrial development and other human activities are the main contributions to the discharge of a high level of heavy metals in water. Thus, their presence in drinking water constitutes a threat to the environment and living organisms' health [23,24]. The affinity for biochar by heavy metals is limited, as a result of the active surface groups generated after the manufacturing process. Therefore, at the present time, the use of physical-chemical pre-treatments of the raw material and post-treatments of the biochar constitutes the main strategy to obtain efficient adsorbents for the treatment of streams polluted with heavy metals. In Table 1 are summarized recent examples of the biochar manufacturing in order to increase the metal adsorption, and in the following subsections, the particularities of the more toxic heavy metals are studied in depth.

Table 1. Recent studies in relation to heavy metal adsorption by different biochars.

Biochar	Temperature (°C)	Procedure	Pollutant	Uptake (mg/g)	Sorption Mechanism	Reference
Montmorillonite modified biochar composites	350	Sodium-montmorillonite and corn straw 1:5, 30 min of ultrasonic dispersion. Neutralization and dried at 80 °C.	Zn	8.16	Chemical interaction	[25]
Iron-impregnated food waste biochar	400	Ratio food waste:FeCl ₃ 1:3, stirring at 60rpm for 24 h.	Se	11.73	Electrostatic interactions	[26]
Corn stalk	600	Mass ratio corn stalk: KOH 4.8:1. Mixture poured in 500 mL Teflon-lined stainless-steel autoclave at 200 °C for 24 h. After cool and dried, pyrolysis at 600 °C for 2 h.	Hg	38.33	Chemical interactions (Hg-O coordination)	[27]
Pomelo peels	500	Pomelo peels: NaOH (5 M) 1:5 (w/v), at 30 °C for 24 h, dried at 60 °C. Pyrolysis under N ₂ atmosphere for 2 h.	Mn	163.19	Chemical adsorption	[28]
Egeria najas (EN)-derived biochar supported nZVI composite	200	EN powder dispersed in SDS alkaline solution at 95 °C for 2 h. Hydrothermal carbonization in 50% glutaraldehyde 8h. nZVI by reducing Fe ²⁺ with KBH ₄ .	Cr(VI)	56.79	Surface complex formation, reduction and ion exchange reaction	[29]
MnO ₂ loaded water hyacinth plants biochar	<700	Nanosized MnO ₂ -loaded biochar was prepared using KMnO ₄ at 25 °C for 30 min, after dropwise addition of 40 mL of 30% H ₂ O ₂ and pH adjusted to 7.0	Pb Cd Cu Zn	268.9 178.2 75.2 68.6	Electrostatic interactions	[30]
3D MnO ₂ modified rice husks biochar	500	Rice husks biochar modified by a rapid redox reaction between KMnO ₄ and Mn(II) acetate and, embedded in the polyacrylamide gel to polymerization	Cd Pb	84.76 70.90	Chemical adsorption	[31]
Jujube pit	800	Pyrolysis under N ₂ atmosphere for 2 h tubular furnace. Immersion MgCl ₂ 0.3M and FeCl ₃ 0.1M (1:100 ratio)	Pb	137.1	Ion exchange	[32]
Grape pomace lignin	700	Feedstock particle size<0.85 mm. From room temperature to 700 °C for 2 h. Sieved < 0.106 mm	Pb	150	Physical and chemical sorption	[33]
Corn Stalks (L-cy/FeOOH@ porous hydrophilic biochar)	120	Mass ratio FeSO ₄ ·7H ₂ O and porous hydrophilic biochar 5:1. Addition of L-cysteine solution and heated in an electric thermostatic drying oven at 120 °C for 12 h.	Pb	103.01	Electrostatic interaction and surface complexation	[34]
Pine sawdust (Magnetic ferrite/biochar composite)	200	Pine sawdust and deionized water heated in Teflon-lined autoclave. Dried material mixture with Mn-Zn ferrites heated to 90 °C and stirred for 1 h. Mass ratio of Mn-Zn ferrites and pine sawdust biochar was 1:1.	Pb	99.5	Chemical binding adsorption, electrostatic attraction and ion exchange	[35]
Amino-modified rice bran biochar/MgFeAlO ₄	210/500	Rice bran and Mili-Qwater 1:12 in a reactor for 5 h at 210 °C. Ratio of Al(NO ₃) ₃ ·9H ₂ O and Mg(NO ₃) ₂ ·6H ₂ O was 1:1.36 and 1:0.70 of FeSO ₄ ·7H ₂ O. Purified and desiccated colloid was calcined in air at 500 °C for 3 h.	Ni	220.75	Physical sorption	[36]
Acoustic pine wood biochar	550–600	Ultrasound by a 20 kHz at 100% amplitude for 30 s and chemical activation by H ₃ PO ₄ (10–30%),	Ni	67%	Chemical interaction	[37]

3.1. Cadmium

Jing et al. [38] reported that the special physicochemical properties of biochar could make it an effective adsorbent in Cd removal, although the mechanism could be different depending on the feedstock or the thermochemical process used [39]. In the recent literature are reported numerous studies that examined the adsorption of Cd by distinctive biochars. Kim et al. [40] found the highest Cd uptake (13.2 mg/g) by biochar produced from *Miscanthus sacchariflorus* at 500 °C. At a high pyrolysis temperature (700 °C), Usman et al. [41] reported that palm biochar increases this level to 43.6 mg/g. However, Teng et al. [42] determined an adsorption maximum of 92.7 mg/g using pinecone biochar prepared at low temperatures (350–400 °C). Based on these previous results, the effect of raw material is remarkable.

Furthermore, in the adsorption process with the increase in pH, the efficiency of Cd removal is augmented. This fact could be explained due to a low pH solution—the large amount of H⁺ in the system protonates the functional groups on the adsorbent surface, which results in the rejection of Cd (II) in the system [41]. However, at a pH higher than 8, the HO⁻ present in the solution could react with Cd, forming low solubility complexes, favoring its precipitation [43].

As depicted in Table 1, methods to improve biochar characteristics could include chemical treatment or the inclusion of metals. In the study by Li et al. [44], they determined that the KMnO₄ impregnation of rape straw biochar enhanced the adsorption capacity, achieving a maximum uptake of 81.10 mg/g. They attributed this enhancement to the increase in specific surface area, the number of oxygen-containing functional groups, and pore size achieved that favor the main mechanisms: cation exchange and cation- π bonding (Figure 3). Akgül et al. [45] reported that among the different composites of tea waste biochar impregnated with Mg, Fe, Mn or Al salts, Mg and Mn biochar composites increased the surface area slightly, being the most efficient in Cd removal. However, these levels have recently been exceeded by Li et al. [46], who evaluated the ability of ZnCl₂, H₃PO₄ and KMnO₄ to modify the *Enteromorpha prolifera*-biochar, showing that the biochar modified with H₃PO₄ considerably increased the uptake (until 423 mg/g) in a short period (\approx 1 h). As has been highlighted in a previous study [47], H₃PO₄ worked as a dehydrating agent, reacting with raw biochar that reduces a substantial amount of hydrogen because of the asymmetric stretching of C–H.

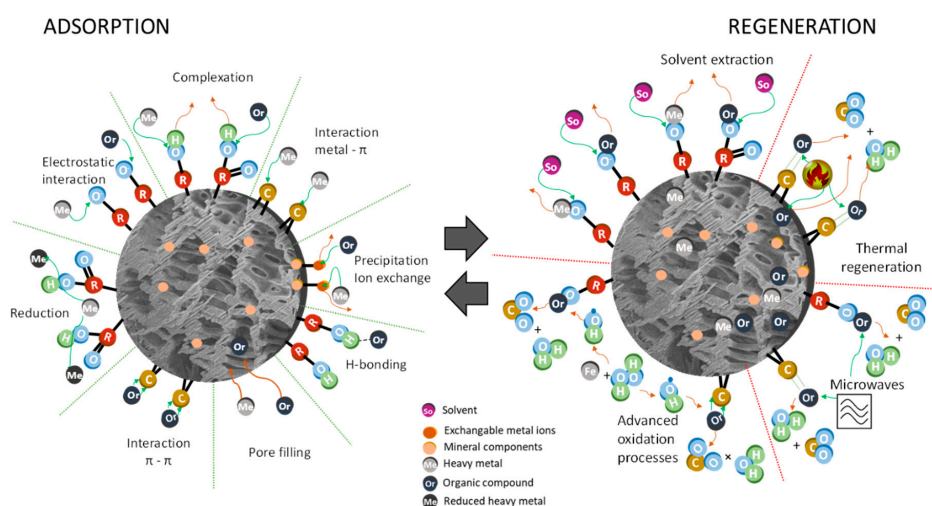


Figure 3. Main sorption mechanisms in biochar (left) and regeneration processes (right).

3.2. Chromium

Cr exists in many valence states, with Cr(IV) being the most soluble of them. In addition, the toxicity of Cr(VI) has been identified as superior to Cr(III) by around 1000 times [48]. Thus, the studies of Cr removal are mainly focused on Cr(IV). As was proposed by Li et al. [49], the adsorption mechanism is by electrostatic attraction and/or reduction to Cr(III) by an oxygen-containing functional group.

In addition, solution pH is recognized as a significant factor in the adsorption process as well as the redox reactions. At pH below the point of zero charge of biochar, the material is positively charged, contributing to the inorganic anions' (HCrO_4^- or $\text{Cr}_2\text{O}_7^{2-}$) negatively charged uptake onto the biochar by electrostatic attraction [50]. However, at low pH, the reduction of Cr(VI) to Cr(III) is favored, thus the electrostatic repulsion can be also generated.

The used feedstock has a great influence in the Cr adsorption mechanism. In several studies using biochar fabricated from sugar beet [51] or coconut coir [52], it was determined that the main mechanism is the Cr(VI) reduction and Cr(III) complexation by hydroxyl and carboxyl groups present in the biochar (Figure 3).

The modification of biochar by metal impregnation can be produced previous to biochar manufacturing. Thus, by hydrothermal carbonization of biomass with metal salts, it is possible to produce a modified hydrochar with a higher surface area, pore volume and aromaticity. Comparison of bamboo sawdust hydrochar modified by ZnCl_2 and AlCl_3 treatment shows a higher C content, reducing the H/C ratio together with an increase in surface area and pore volume, with biochar modified by ZnCl_2 achieving the best result (Cr(VI) uptake 14 mg/g), with levels around three-fold higher in relation unmodified biochar [53]. In addition, cations added on the surface may have enhanced electrostatic interaction between Cr(VI) and the adsorbent. Similarly, Sun et al. [54] prepared several iron–biochar composites with different Fe/biochar ratios, by pyrolysis at 1000 °C of pre-treated forestry wood waste with FeCl_3 . The XPS analyses of spent biochar showed that as Fe loading increases, the dominating specie is FeCr_2O_4 (78.7% at a loading of 2:1), suggesting the reduction of Cr(VI) by Fe^0 .

Recently, porous biochar was successfully improved by chemical activation of KOH [55], increasing the specific surface area, micropore distribution and pore diameters (1–2 nm). This modified biochar presented an excellent adsorption performance with a theoretical monolayer uptake of 116.97 mg/g for Cr(VI), operating at acid pH below the point of zero charge.

3.3. Mercury

Until now, few studies have reported Hg adsorption by biochar. Two biochars from bagasse and hickory chips were synthesized by Xu et al. [56], revealing that surface complexation and cation- π bonding on biochar are the most important mechanisms in the Hg adsorption (Figure 3). Liu et al. [57] produced thirty-six biochars from wood, agricultural residue, and manure feedstocks at 300 and 600 °C. They concluded the preference of Hg to bind to sulfur atoms when its level is high in the biochar, while at a low level, Hg is bound to oxygen and chlorine functional groups. Thus, sulfurized biochar enhances Hg removal by forming a Hg-S bond [58]. In this context, biochars produced from tobacco, rice and wheat were treated with H_2S , showing the play role of C-S functional group in the adsorption process that is increased more than seven-fold compared to the level achieved in unmodified biochar [59]. Similarly, biochars produced by pyrolysis (range temperature 300–900 °C) from poplar wood were able to remove Hg from water, although their modification with FeCl_3 and FeSO_4 increased the Hg removal due to the contribution of adsorbing sites of Fe^0 , Fe_{1-x}S , and Fe_2O_3 [60].

Another new alternative is the application of microwave activation to increase the porosity of the adsorbent. In this framework, Shan et al. [61] prepared biochar from cotton straw by “microwave activation and Mn-Fe mixed oxides impregnation assisted by ultrasound treatment”. The combination of these techniques allows for increasing its porosity, and ultrasound favors Mn and Fe distribution in the biochar composite.

Recently, biochar produced by pyrolysis of high-salinity *Spirulina* residue in a temperature range from 350 to 700 °C for 90 min (heating rate of 15 °C/min) shows excellent sorption of Hg (uptake ranged from 107.1 to 196.1 mg/g), which is mainly due to the high content of nitrogen, sulphur-heterocycles and chlorine-containing minerals formed in the biochar production. The results are in agreement with previous studies, in which by the use of a nitrogen-doped microalgae biochar, Hg sorption was enhanced [62].

3.4. Lead

In the literature, various kinds of biochar have been used for the removal of lead. Thus, Lee et al. [63] determined the high adsorption capability of three unmodified biochars produced

from peanut shell, ginkgo and metasequoia leaf. However, better results were reached by rice straw biochar prepared by pyrolysis at 700 °C (Pb uptake 171.34 mg/g) [64].

Likewise, Pb removal using the biochar produced from different feedstocks (peanut shells, corn cobs, poultry manure, buckwheat husk, and white mulberry wood) was considerably high above 97.5% [65]. This fact could be attributed to four adsorption mechanisms driven by the main biochar properties, such as organic functional groups, mineral content, ionic content and π -electrons (Figure 3). These sorption mechanisms may take place simultaneously or supplementing each other.

Gao et al. [32] studied the Pb adsorption by jujube (*Ziziphus jujuba*) pit biochar, determining the positive effect by increasing the pH of the solution and the influence of coexisting ions, such as K^+ and Na^+ . In addition, the reusability of the biochar was measured for five cycles. The regeneration process was done by solvent extraction (Figure 3) using 0.2 M hydrochloric acid and washed using distilled water followed by drying. It is detected that the removal level was around 70% of the initial adsorption capacity after the last round; this procedure can reduce the operational cost of the adsorption process.

To improve the Pb adsorption capability of biochar, several treatments of biochar have been proposed, such as alkali [66] or acid treatment, [67] chemical modification with ammonia, hydrogen peroxide and nitric acid [68] and chemical graft [69]. Recently, Zhang et al. [30] used the redox precipitation method to load manganese dioxide (MnO_2) nanoparticles on invasive water hyacinth biochar produced by pyrolysis at 450 °C at 5 °C/min. They determined higher calculated maximum uptakes (216.22–351.37 mg/g) concerning other biochars. Based on the kinetic study, it was determined that the rate-limiting step is chemisorption, Langmuir model represents the isotherm model, and Pb was adsorbed onto biochar via carbonyl and hydroxyl groups. Thus, the high Pb uptakes decreased when the concentration of coexistent natural cations common present in wastewater or natural water, such as K^+ , Na^+ , Ca^+ , and Mg^{2+} , was increased.

In this line, Ifthikar et al. [70] reported a facile one-pot synthesis technique to obtain a carboxymethyl chitosan coating on sewage sludge biochar with Pb and Hg removal capacity and good reusability. The modified biochar showed shorter equilibrium time for Pb and Hg adsorption with a capacity of 210 and 594.17 mg/g, respectively, a fact that could be explained by the strong chemical interactions between the amino, hydroxyl and carboxyl functional groups present in the modified biochar and heavy metals. Likewise, the adsorbent exhibited good stability, its regeneration being made possible by the use of Na_2 -EDTA solution (0.05M) as a regenerative agent without significant biochar alteration after five regeneration cycles, keeping a similar adsorption capacity.

4. Biochar Adsorption of Emerging Contaminants

Presently, the so-called “emerging contaminants” as the result of anthropogenic activities are being released into the environment and have been detected in surface water, groundwater, drinking water and wastewater treatment plant effluents in trace amounts. In recent years, the development of new and more sensitive methods of analysis has made it possible to alert people to the presence of these micropollutants. Just in the case of Europe, more than 700 of these compounds have been reported [71]. Thus, a standard pharmaceutical product such as ibuprofen has been detected in several scenarios, such as wastewater treatment plant effluents (0.038 μ g/L) [72], surface water (6–780 ng/L) [73], groundwater (4–2250 ng/L), and drinking water (4–50 ng/L) [74]. In the same scenarios, it is also possible to find pesticides such as atrazine in surface water (1.29 μ g/L) [75] or dyes such as disperse blue 373 or disperse red 1 in the effluents of a wastewater treatment plant in a range of 0.03–0.35 μ g/L [76]. These facts confirm that the current wastewater treatment plants are not designed to remove these micropollutants.

In this context, it should be noted that one of the main handicaps for proper treatment is their low concentration, and the adsorption process stands out. However, the large variety of micropollutants requires the design of new and more specific adsorbents, so the use of unmodified or modified biochar opens up a field of possibilities. In Table 2, the recent research on the application of biochar in the restoration of aquatic environments containing several organic contaminants is summarized.

Table 2. Organic pollutants adsorption by different unmodified and modified biochars.

Biochar	Pyrolysis	Procedure	Pollutant	N (%)	H (%)	O (%)	C (%)	Surface Area (m ² /g)	Isotherm Model	Uptake (mg/g)/ Maximum Removal (%)	Sorption Mechanism	Ref.
Kraft lignin	500 °C for 1 h under an N ₂ flow (100 mL/min)	Kraft lignin washed with 1% H ₂ SO ₄ solution and impregnated with H ₃ PO ₄ solution (85% w/w) at 85 °C for 6 h, using an H ₃ PO ₄ : lignin weight ratio of 1.4. Dried slurry at 105 °C for 2 d	Bisphenol A	0.26	3.04	34.67	61.45	1053	Dual-site Langmuir	195.5	Intra-particle diffusion	[77]
Spherical biochars (derived from pure glucose)	900 °C lid-enclosed porcelain crucible for 3 h in a non-circulated air atmosphere.	Two-stage process: hydrothermal carbonization (190 °C and 24 h) of glucose solution (125 g/L) in Teflon autoclave and pyrolysis 900 °C	Paracetamol	0	0	19.9	80.1	1292	Redlich–Peterson	286	π - π interactions and Van der Waals force	[78]
Cotton straw	350 °C under oxygen-free conditions	Aged biochar in air over 12 months prior to use	Sulfamethoxazole N ₄ -acetyl-sulfamethoxazole	0.37	1.04	n.a	31.22	68.4	n.a	38% 61%	π - π interaction	[79]
Swine manure	600 °C 2h with N ₂ purge	Dried at 60 °C for 24 h and pulverized and screened by a 100-mesh sieve.	Sulfamethazine	2.34	1.45	14.21	52.36	9.15	Langmuir—Hinshelwood	80.2%	Electrostatic attraction	[80]
Pomelo peel	600 °C for 2h with a heating rate of 10 °C/min	Biochar: KOH at a mass ratio of 1:4. Activation: wash with 35% HNO ₃ for 24 h. Dried at 80 °C for 24 h and sieved <75 μ m	Tetracycline	n.a	n.a	11.81	86.18	2457.37	Langmuir	476.2	π - π interactions	[81]
Fallen maple leaves	750 °C under constant N ₂ atmosphere for 2 h	Pulverized maple leaves (500 and 2360 μ m). Biochar sieved below 106 μ m	Tetracycline	0.74	0.80	16.63	42.15	191.1	Freundlich	407.3	Chemical sorption	[82]
Wheat stalk	600 °C 4h N ₂ atmosphere	Dried at 105 °C and sieved 0.15–0.45 mm. Ball-milled ratio 1:100 Biochar: ball mass	Tetracycline	n.a	n.a	n.a	n.a	257.50	Langmuir	84.54	Electrostatic attraction	[83]
Bamboo sawdust	450 °C 5 h	Dried at 80 °C and biochar crushed-sieved 100-mesh. Effect of citric acid and Ca ²⁺	Tetracycline	0.62	3.41	17.87	75.09	140.51	Langmuir	15.4		[84]
Rice straw	300 °C 1h O ₂ -limited conditions	Alkali-acid combined and magnetization method by co-precipitation with Fe ²⁺ /Fe ³⁺ solution (1:1), slowly stirred at 60°C for 30 min.	Tetracycline	0.73	1.74	24.30	43.49	140.1	Freundlich	98.3	Electrostatic attraction	[85]

Table 2. Cont.

Biochar	Pyrolysis	Procedure	Pollutant	N (%)	H (%)	O (%)	C (%)	Surface Area (m ² /g)	Isotherm Model	Uptake (mg/g)/ Maximum Removal (%)	Sorption Mechanism	Ref.
Peanut shell	400 °C 4h under N ₂ atmosphere	Dried and crushed into fragments of 0.2–0.6 mm. Fe ₂ O ₃ was premixed with crushed peanut shell at about 11% (w/w) for 24 h. Biochar crushed and sieved (0.150 mm).	Methylene Blue Acid Orange 7	1.14	2.80	28.9	52.4	13.7	n.a	92.4% 85.1%	π-π interactions	[86]
Wheat straw	700 °C for 4 h (3 °C/min)	Mg:Al molar ratio 0.003:0.001. Ratio mass of biochar and mixture of Mg: Al 1:2.3. Sonicated for 1 h	Methylene Blue	n.a	n.a	n.a	n.a	441.06	Langmuir	302.75	Electrostatic attraction and π-π interactions	[87]
Sawdust biochar	700 °C for 2 h (15 °C/min) under N ₂ atmosphere	Washed, dried, crushed, and sieved into 0.149 mm sieve	Acid Orange 7	n.a	4.38	n.a	67.0	311	n.a	21.3%	Electrostatic attraction	[88]
Orange peels	Microwave pyrolysis Rapid heating rate (15–120 °C/min), higher temperature (>800 °C) 15 min	Dried 105 °C for 24 h and crushed into 4 mm. Combines microwave heating and activation by CO ₂ or steam	Congo Red dye	0.5	2.1	19.0	783.4	158.5	Freundlich	136	Electrostatic attraction	[89]
Waste tea residue	700 °C slow pyrolysis for 2 h (7 °C/min) under limited O ₂	Ground into particles ≤0.1 mm Activation under a flow of steam at 5 mL/min for 45 min at the peak temperature 700 °C and atmospheric pressure	Caffeine	2.5	n.a	8.37	87.67	576.06	Freundlich	15.4	π-π and hydrogen bonding interactions	[90]

n.a.: not available.

These results confirm that biochar produced in the laboratory can adsorb organic pollutants at a similar level to commercial activated carbon. As an additional advantage, the regeneration of biochar can be easily carried out through different treatments (Figure 3), such as microwave irradiation, thermal or chemical treatment [91–93], including by extraction with organic solvents or by direct degradation on the biochar surface using advanced oxidation processes [94–96].

The adsorption mechanism to remove organic compounds depends on the nature of the pollutants and the properties of biochar, which vary greatly with the selected feedstock and the thermochemical process used. For example, when the temperature is increased, the aromaticity, hydrophobicity and surface area of biochar also increase, which makes it a suitable adsorbent for hydrophobic organic compounds. In addition, by application of other traditional or emerging technologies (such as coating, physical or chemical activation, nanotechnology and/or biotechnology) it is possible to create additional active sites to favor the removal of these organic pollutants [75,76]. Therefore, due to the diversity of synthesized biochar as well as the variety of organic compounds with different properties, the recent developments in this issue focusing on the most abundant organic contaminants (dyes, pharmaceuticals and personal care products) are summarized.

4.1. Dyes

In the literature, a multitude of studies have been reported in which the biochar has been manufactured from different feedstocks, evaluating the effect of the pyrolysis parameter in its dye adsorption capacity [97,98]. Thus, recent improvements in different biochars to enhance the adsorptive properties of the biochar will be presented.

One alternative is the use of ball-milling technology, which offers advantages such as consuming less energy, not requiring chemicals during the ball-milling process and increasing the specific surface area of biochar by 65 times [99]. Lyu et al. [100] applied this technology in a planetary ball mill to sugarcane bagasse biochar to increase its sorption ability to a soluble cationic dye, methylene blue. The reported results reveal that this technology increases the external and internal surface area, oxygen-containing functional groups and reduces the point of zero charges from 4.2 to 2.7, thereby enhancing methylene blue adsorption via π - π interaction and electrostatic attraction (Figure 3).

As was reported by Inyang et al. [101], the increase in oxygen species on the surface of biochar by incorporation of carboxylic, carbonyl, lactonic, and phenolic groups affects the dye removal. In this sense, several strong acids (HNO_3 , KMnO_4 , H_2O_2 , H_3PO_4 or HCl) have been tested, with a positive effect on biochar adsorptive properties [102]. The biochar modification process could be improved by combination with other agents. Thus, methylene blue was also removed by bamboo hydrochar modified with HCl and NaOH [103]. By a sequential acid/ NaOH treatment, it is possible to enlarge the surface area and pore volume of hydrochar in the first stage, followed by the enhancement of the oxygen-containing functional groups by the activation process with NaOH . In addition, it was concluded that by activation, the π - π interactions could be considered as the primary mechanism, and electrostatic attraction and ion-exchange mechanism interactions between cationic dye and hydrochars are also involved.

Another alternative is the use of activating agents (such as ammonium chloride or ammonium acetate) to produce nitrogen-doped biochar due to the binding with carbon and generating nitrogen-containing functional groups during the heating process (such as nitrogen-pyrrole, nitrogen-pyridine, or nitrogen-oxidized). In a comparative study of nitrogen-doped biochar with one derived from phosphoric acid activation for the removal of an azo dye, acid red 18, the authors concluded that maximum adsorption capacity increased by 40% due to the beneficial effect of N- functional [104]. To obtain similar nitrogen-doped biochar, Xu et al. [105] applied a simple method by ball-milling bagasse biochar with ammonium hydroxide. In this case, it was detected that the nitrogen species were amine and nitrile, whose presence enhanced the sorption of the dye reactive red to 16 times the level of unmodified biochar.

New composites have been produced satisfactorily by the co-precipitation method, such as MgAl-layered double hydroxide (LDH) bovine bone biochar composite. Meili et al. [106] tested this composite in the adsorption of methylene blue, achieving uptake around 406 mg/g, with the capacity for solvent regeneration with methanol and sodium chloride (Figure 3). However, the efficiency of adsorbent decreases until uptake around 70 mg/g after six cycles due to the disintegration of LDH. Better results were obtained when a green banana peel biochar/iron oxide composite was manufactured, enhancing its adsorb dye capacity in a wide range of pH, keeping the uptake level after five regeneration cycles [107]. Similarly, a novel Fe₃O₄-graphene-biochar composite (GBC-Fe₃O₄) was prepared for the removal of crystal violet dye. In this composite, the introduction of graphene and Fe₃O₄ nanoparticles reduced the zeta potentials and the mechanism study suggested the interactions of functional groups, such as aromatic C=C and C=O, -OH, C-C, and π - π interactions played an important role in dye adsorption [108].

4.2. Pharmaceuticals and Personal Care Products (PPCPs)

Due to drug abuse, the concentration of this kind of pollutant in several water scenarios far exceeds the pollution limit, so there is an urgent need for a potentially efficient, sustainable and eco-friendly method such as biochar adsorption to avoid this problem. Thus, to obtain a stable and repeatable adsorbent with better pollutant removal efficiency, it is necessary to prepare engineered biochar by the application of modification techniques such as metal embedding, nanomaterial decoration or surface functionalisation.

In this context, by hydrothermal treatment, hierarchical MoS₂ nanomaterials were embedded in rice straw biochar, obtaining a novel biochar-based nanomaterial “g-MoS₂ nanosheet-decorated biochar” that was tested in the removal of tetracycline hydrochloride [109]. The pore structures and surface properties of biochar enhanced the tetracycline hydrochloride adsorption by several binding mechanisms: electrostatic interaction, pore-filling, hydrogen bonding and π - π conjugate effect (Figure 3). In addition, this material showed excellent reusability, as NaOH treatment detected only a slight reduction after five adsorption/desorption cycles.

In the literature, different metal-biochar composites have been synthesized, providing good results thanks to their multifunctionality (adsorption, reduction, and catalytic activity) that make them good materials for the removal of different contaminants [110]. Cho et al. [111] prepared by pyrolysis a “multifunctional mixed metal-biochar composites” using a mixture of two abundant industrial wastes, red mud and lignin, and demonstrated its ability to perform the removal of p-nitrophenol and p-chlorobenzoic acid and a great variety of contaminants.

The removal of bisphenol A and sulfamethoxazole was successfully performed by adsorption on a “biochar-supported magnetic CuZnFe₂O₄ composite” [112]. The involved mechanisms were charge-assisted H-bonding, hydrophobic, and π - π electron donor-acceptor interactions. The main advantages of this composite are its magnetic properties, which made the separation process easy and reduced the reusability to lower than 10% after four cycles of regeneration, as well as the removal efficiency of both pollutants.

Another conventional process such as the physical and chemical activation of the biochar also allows for obtaining substantial improvements in the material properties that favor the removal of pharmaceuticals and personal care products [113]. Thus, steam and phosphoric acid can activate the surface of bagasse biochar at high temperature, creating many holes on the surface, thereby increasing the adsorption of ibuprofen [114]. In addition, this biochar presented reusability potential by ibuprofen desorbing with methanol, but after four adsorption/desorption cycles, the removal percentage decreased by around 30%.

5. Limitation of Biochar Application

In the production of biochar by thermochemical technologies the reduction in the waste volume is also possible, as well as the complete destruction of pathogens and parasites, immobilizing metals

and producing value-added bio-energy. However, the presence of impurities, mainly heavy metals, which are part of the wastes used as feedstock, may be a risk due to the heavy metals leaching during biochar application. Recently, a few papers have reported the behavior of heavy metals during the pyrolysis process, focusing on their distribution and mobility in the biochar [115]. Shen et al. [116] studied the transformation behaviors of heavy metals in animal manure during pyrolysis at 300–700 °C. The results indicate that the characteristics of biochars (>500 °C) were relatively stable. Under this condition, the total percentages decreased from 16.98% to 9.43% for Cr, 85.60% to 65.55% for Mn, 57.26% to 10.61% for Cu, and 37.90% to 13.78% for Zn, respectively, determining that the bioavailability and toxicity of Cr, Mn, Cu and Zn in pig manure biochar were greatly reduced and the potential ecological risk index values significantly decreased after pyrolysis. Additionally, to reduce their possible adverse effects, one solution is the mixture of different kinds of biomass. Thus, co-pyrolysis of animal manures and biomass with lower heavy metals contents may lead to a decrease in the heavy metal contents in the obtained biochar compared to the single manure pyrolysis [117,118]. By co-pyrolysis, it is possible to convert the more toxic heavy metals into stable fractions with a significant reduction in their bioavailability in biochar [119]. Huang et al. [117] reported a minimal effect on the mobility of different heavy metals in biochar by the co-pyrolysis process of a mixture of sewage sludge with rice straw or sawdust at 50% mixture ratio. Similarly, Jin et al. [120] detected the transformation of unstable metals into more stable fractions at a 50% mixture ratio of bamboo sawdust and sludge pyrolysis. Hence, the resultant biochars and their chemical composition depend on the kind of feedstock used and the controlling rate of pyrolysis temperature or the use of a mixture of feedstocks [121].

6. Regeneration of Biochar

The desorption process for the recovery of the biochar is of extreme importance in assessing their potential to be reused. The metal recovery of a solution may be based in different mechanisms (precipitation, complexation or ion exchange) [122]. Solvent regeneration achieves the pollutant desorption from biochar, taking into account the equilibrium relationship between biochar, the solvent and pollutant to break the adsorption equilibrium by changing the temperature and the pH value of the solvent [123].

Different acids and bases (NaOH, HCl, H₂SO₄, EDTA, HNO₃, Ca(NO₃)₂, NaNO₃) are used as reagents for desorbing [124]. Thus, alkaline regeneration agents, such as NaOH, NaHCO₃, and NaH₂PO₄, have been found to efficiently desorb As from Fe-impregnated biochar [125]. Additionally, 0.1 M NaOH is able to desorb 72% of initially sorbed As(V) on biochar, showing that desorption and regeneration rates decreased gradually with the number of cycles, from 72% (the first cycle) to 60% (the third cycle) [125]. Similarly, Fe₃O₄@-orange peel can be recycled using 0.1 M HNO₃ with a desorption capacity of 98.5% after five recycling cycles [126]. The efficacy of recycling biochar using different organic solvents was examined in several studies. Reguyal et al. [95] revealed that methanol, ethanol, and acetone have a higher regeneration capacity by separation of organic contaminants from the biochar.

Another alternative to achieve the pollutant desorption from biochar is the thermal method or microwave irradiation in which the adsorbed pollutant is carbonized and decomposed and eventually the molecule becomes smaller than the pore size of biochar and escapes [123]. In thermal regeneration, there is a relationship between the temperature and the regeneration efficiency—for example, when *Enteromorpha prolifera* biochar polluted by pyrene was regenerated at 80, 150, and 200 °C, the regeneration efficiency was 35.00%, 45.00% and 48.00%, respectively [127]. In the microwave irradiation method, the trapped polar substance molecules in biochar are used to produce dipole to polarization and the electromagnetic field can be transformed into heat energy, generating the heating and volatilization of the organic substances present in the biochar. The main advantage of this method over thermal method is the uniform heating of the biochar, preserving its porous structure [128].

Latterly, the combination of treatment processes has led to improved treatment techniques due to the synergistic effect between them. Among the different alternatives, advanced oxidation

processes (AOPs) have been demonstrated to be effective for removing organic pollutants from wastewater [129,130]. Recently, in the literature several processes have been reported in which the biochar is used as a catalyst to AOPs or the AOPs are applied to the exhausted biochar regeneration. Thus, Li et al. [131] synthesized a Fe, N co-doped wheat straw biochar using urea, and ferrous sulfate as precursors and apply to activate persulfate for organic contaminant degradation (such as acid orange, methyl orange, phenol, bisphenol A and tetracycline hydrochloride). In this line, Mer et al. [132] suggested a dual application of biochar as an adsorbent of nickel and lead and subsequent degradation of phenol through in situ generation of hydroxyl radicals. Zhang et al. [133] concluded that the defective structures and functional groups (C-OH) of mesoporous biochar (by bagasse calcination with KOH and CaCl₂ modified activation) to act as reaction active sites which played important roles in the oxidative degradation of phenol.

Thus, in the degradation of sulfamethoxazole by persulfate activation, Lykoudi et al. [134] figured out a clear linear relationship between the spent-coffee biochar activity and the sodium persulfate concentration, and the process is favored by the adsorption of sulfamethoxazole on the biochar surface. Similarly, Acevedo-García et al. [94] demonstrated the high adsorption capacity of lime fiber biochar by the removal of sulfamethoxazole and methylparaben and its feasible regeneration by several alternative AOPs (Fenton, electro-oxidation-H₂O₂ and electro-Fenton).

To sum up, in this kind of process, biochar is a key factor as an adsorbent and catalyst or activator. This synergic effect increases the efficiency of the degradation process and demonstrates the potential application of biochar as a cost-effective agent to treat organic pollutant wastewater.

7. Economic Analysis and Future Prospects

The cost analysis is an important aspect to evaluate the production and implementation of the proposed materials. The global biochar market was USD 1.39 billion in 2019, and it is expected to increase to USD 3.46 billion in 2025. This product is mainly used in agriculture application (71.1% in 2018), but other areas such as water and wastewater treatment have shown an increase in the demand of the products, mainly in emerging economies [135]. There are several processes for the production of the biochar as it is displayed in Figure 2, but pyrolysis is the most effective process actually used.

Biochar obtained by pyrolysis presents excellent adsorptive properties for organic and inorganic compounds, which suggests an increase in this use in the near future and can be considered as a feasible cheaper alternative to the more expensive activated carbons. Krasucka et al. [136] reported a biochar production cost of 350–1200 USD/ton, which is lower than the reported value for activated carbon—USD 1100–1700 per ton. Other studies showed even lower biochar production prices as 90 USD/ton in the Philippines and higher values for those produced in the UK, at 8850 USD/ton [137]. From an economic point of view, the market price of the biochar depends on the effectiveness of the generated material and is an important factor correlated with the biochar cost. Moreover, several aspects related to biochar production, such as the selected feedstock, pyrolysis production conditions and transport, considerably affect the production costs. Homagain et al. [138], using life cycle assessment analysis, reported that most of the production cost is related to the pyrolysis process, but also significant cost is related to the storage/processing of the biochar and feedstock. Similarly, Keske et al. [139] considered these aspects in their economic analysis of biochar production from Canadian black spruce forest. The reported results imply that the pyrolysis stage is the most costly, attaining 36% of the cost, followed by feedstock collection (12%) and transportation cost (9%), which resulted in a biochar cost of 762.20 USD/ton. Thus, the reduction in the cost may rely on the use of new production technologies and the selection of appropriate and suitable low-cost materials. The use of wastes is aligned with circular economy principles and the goals of “2030 Agenda for Sustainable Development” adopted by the United Nations for reducing carbon emissions, favoring the reuse of materials and avoiding the generation of waste.

The future prospects of biochar require researchers to face several challenges associated with these materials for proper use. One of these challenges is the search for potential feedstock materials and wastes as low-cost materials for the production process attaining good adsorptive properties. Based on this, the design of engineered biochar adsorbents (via activation) for the removal of specific compounds is also required due to the wide variety of pollutants that are being released to the environment. The management of the spent biochar adsorbents by regeneration is another aspect to be considered and is required to tackle with. All these issues also require the performance of an economic analysis of the biochar production including activation and regeneration costs, which is an important factor to be considered in the development of these biochars and have been scarcely studied.

8. Conclusions

The problems derived from the presence in the aquatic environment of heavy metals, which are not susceptible to degradation, and organic pollutants, usually characterized by their low concentration, request the application of separation technology, such as adsorption. In this review, the recent advances in the efficient production of engineering biochar that increase the application of adsorption process as the primary separation technology are highlighted. The production and modification of biochar produced from biomass wastes open up new paths for the production of engineered adsorbents and demonstrate advantages over commercial activated carbon. The feedstock and biochar manufacturing process (operating conditions, pre or post physical-chemical treatments) have demonstrated to meaningful influence over the removal of the pollutants attaining upright removal efficiencies. The synthesis of the biochar according to the target pollutant is postulated to be a next step in the research. Thus, the introduction of metals, chemical treatment and so forth attained a significant adsorption enhancement in the removal of organic and metallic pollutants caused by the increase in the surface area, pore area and reactivity of the adsorbent. Furthermore, the probed regeneration of these carbonaceous materials increases the usability of these renewable sources for the treatment of huge amounts of wastewater. However, experimental and modelling studies in packed columns are highly recommended for future studies in order to validate the real use and scalability of the synthesized biochars.

Author Contributions: Conceptualization, A.F.-S.; formal analysis, A.F.-S.; data curation, A.F.-S., E.R.; writing—original draft preparation, A.F.-S., E.R.; writing—review and editing, M.A.S.; visualization, M.P.; supervision, M.A.S. and M.P.; project administration, E.R.; funding acquisition, M.A.S. and M.P. All authors have read and agreed to the published version of the manuscript.

Funding: This work was supported by the Spanish Ministry of Science, Innovation and Universities, Xunta de Galicia and ERDF (Grant No. CTM2017-87326-R and ED431C 2017/47).

Conflicts of Interest: The authors declare no conflict of interest. The funders had no role in the design of the study; in the collection, analyses, or interpretation of data; in the writing of the manuscript, or in the decision to publish the results.

References

1. Ahmad, B.; Yadav, V.; Yadav, A.; Rahman, M.U.; Yuan, W.Z.; Li, Z.; Wang, X. Integrated biorefinery approach to valorise winery waste: A review from waste to energy perspectives. *Sci. Total Environ.* **2020**, *719*. [[CrossRef](#)]
2. Ricciardi, P.; Cillari, G.; Carnevale Miino, M.; Collivignarelli, M.C. Valorization of agro-industry residues in the building and environmental sector: A review. *Waste Manag. Res.* **2020**, *38*, 487–513. [[CrossRef](#)]
3. Bora, R.R.; Tao, Y.; Lehmann, J.; Tester, J.W.; Richardson, R.E.; You, F. Techno-Economic Feasibility and Spatial Analysis of Thermochemical Conversion Pathways for Regional Poultry Waste Valorization. *Acs Sustain. Chem. Eng.* **2020**, *8*, 5763–5775. [[CrossRef](#)]
4. Lehmann, J.; Joseph, S. *Biochar for Environmental Management: Science and Technology*; Wiley: New York, NY, USA, 2012; ISBN 9781849770552.
5. Zabaniotou, A.; Stavropoulos, G.; Skoulou, V. Activated carbon from olive kernels in a two-stage process: Industrial improvement. *Bioresour. Technol.* **2008**, *99*, 320–326. [[CrossRef](#)]

6. El-Naggar, A.; El-Naggar, A.H.; Shaheen, S.M.; Sarkar, B.; Chang, S.X.; Tsang, D.C.W.; Rinklebe, J.; Ok, Y.S. Biochar composition-dependent impacts on soil nutrient release, carbon mineralisation, and potential environmental risk: A review. *J. Environ. Manag.* **2019**, *241*, 458–467. [[CrossRef](#)]
7. Yang, X.; Wan, Y.; Zheng, Y.; He, F.; Yu, Z.; Huang, J.; Wang, H.; Ok, Y.S.; Jiang, Y.; Gao, B. Surface functional groups of carbon-based adsorbents and their roles in the removal of heavy metals from aqueous solutions: A critical review. *Chem. Eng. J.* **2019**, *366*, 608–621. [[CrossRef](#)]
8. Xiao, X.; Chen, B.; Chen, Z.; Zhu, L.; Schnoor, J.L. Insight into Multiple and Multilevel Structures of Biochars and Their Potential Environmental Applications: A Critical Review. *Environ. Sci. Technol.* **2018**, *52*, 5027–5047. [[CrossRef](#)]
9. Ahmad, M.; Rajapaksha, A.U.; Lim, J.E.; Zhang, M.; Bolan, N.; Mohan, D.; Vithanage, M.; Lee, S.S.; Ok, Y.S. Biochar as a sorbent for contaminant management in soil and water: A review. *Chemosphere* **2014**, *99*, 19–33. [[CrossRef](#)] [[PubMed](#)]
10. Rosales, E.; Meijide, J.; Pazos, M.; Sanromán, M.A. Challenges and recent advances in biochar as low-cost biosorbent: From batch assays to continuous-flow systems. *Bioresour. Technol.* **2017**, *246*, 176–192. [[CrossRef](#)]
11. Do Minh, T.; Song, J.; Deb, A.; Cha, L.; Srivastava, V.; Sillanpää, M. Biochar based catalysts for the abatement of emerging pollutants: A review. *Chem. Eng. J.* **2020**, *394*. [[CrossRef](#)]
12. Zhang, C.; Zhang, Z.; Zhang, L.; Li, Q.; Li, C.; Chen, G.; Zhang, S.; Liu, Q.; Hu, X. Evolution of the functionalities and structures of biochar in pyrolysis of poplar in a wide temperature range. *Bioresour. Technol.* **2020**, *304*, 123002. [[CrossRef](#)] [[PubMed](#)]
13. United Nations, Department of Economic and Social Affairs. *P.D. World Population Prospects: The 2010 Revision, Highlights and Advance Tables 2011*; ESA/P/WP.220; New York US United Nations, Department of Economic and Social Affairs: New York, NY, USA, 2010.
14. Crini, G.; Torri, G.; Lichtfouse, E.; Kyzas, G.Z.; Wilson, L.D.; Morin-Crini, N. Dye removal by biosorption using cross-linked chitosan-based hydrogels. *Environ. Chem. Lett.* **2019**, *17*, 1645–1666. [[CrossRef](#)]
15. Pires, J.; Pinto, M.L.; Carvalho, A.; De Carvalho, M.B. Assessment of Hydrophobic-Hydrophilic Properties of Microporous Materials from Water Adsorption Isotherms. *Adsorption* **2003**, *9*, 303–309. [[CrossRef](#)]
16. Han, Y.; Cao, X.; Ouyang, X.; Sohi, S.P.; Chen, J. Adsorption kinetics of magnetic biochar derived from peanut hull on removal of Cr (VI) from aqueous solution: Effects of production conditions and particle size. *Chemosphere* **2016**, *145*, 336–341. [[CrossRef](#)]
17. Xiang, W.; Zhang, X.; Chen, J.; Zou, W.; He, F.; Hu, X.; Tsang, D.C.W.; Ok, Y.S.; Gao, B. Biochar technology in wastewater treatment: A critical review. *Chemosphere* **2020**, *252*, 126539. [[CrossRef](#)]
18. Yang, H.; Ye, S.; Zeng, Z.; Zeng, G.; Tan, X.; Xiao, R.; Wang, J.; Song, B.; Du, L.; Qin, M.; et al. Utilisation of biochar for resource recovery from water: A review. *Chem. Eng. J.* **2020**, *397*. [[CrossRef](#)]
19. Yoder, J.; Galinato, S.; Granatstein, D.; Garcia-Pérez, M. Economic tradeoff between biochar and bio-oil production via pyrolysis. *Biomass Bioenergy* **2011**, *35*, 1851–1862. [[CrossRef](#)]
20. Yao, Y.; Gao, B.; Zhang, M.; Inyang, M.; Zimmerman, A.R. Effect of biochar amendment on sorption and leaching of nitrate, ammonium, and phosphate in a sandy soil. *Chemosphere* **2012**, *89*, 1467–1471. [[CrossRef](#)]
21. Kwon, G.; Bhatnagar, A.; Wang, H.; Kwon, E.E.; Song, H. A review of recent advancements in utilisation of biomass and industrial wastes into engineered biochar. *J. Hazard. Mater.* **2020**, *400*. [[CrossRef](#)] [[PubMed](#)]
22. Li, Y.; Xing, B.; Ding, Y.; Han, X.; Wang, S. A critical review of the production and advanced utilisation of biochar via selective pyrolysis of lignocellulosic biomass. *Bioresour. Technol.* **2020**. [[CrossRef](#)]
23. Neeli, S.T.; Ramsurn, H.; Ng, C.Y.; Wang, Y.; Lu, J. Removal of Cr (VI), As (V), Cu (II), and Pb (II) using cellulose biochar supported iron nanoparticles: A kinetic and mechanistic study. *J. Environ. Chem. Eng.* **2020**, *8*, 103886. [[CrossRef](#)]
24. Liu, M.; Li, X.; He, Y.; Li, H. Aquatic toxicity of heavy metal-containing wastewater effluent treated using vertical flow constructed wetlands. *Sci. Total Environ.* **2020**, *727*, 138616. [[CrossRef](#)]
25. Song, J.; Zhang, S.; Li, G.; Du, Q.; Yang, F. Preparation of montmorillonite modified biochar with various temperatures and their mechanism for Zn ion removal. *J. Hazard. Mater.* **2020**, *391*, 121692. [[CrossRef](#)] [[PubMed](#)]
26. Hong, S.H.; Lyonga, F.N.; Kang, J.K.; Seo, E.J.; Lee, C.G.; Jeong, S.; Hong, S.G.; Park, S.J. Synthesis of Fe-impregnated biochar from food waste for Selenium(VI) removal from aqueous solution through adsorption: Process optimisation and assessment. *Chemosphere* **2020**, *252*, 126475. [[CrossRef](#)]

27. Zhang, S.; Song, J.; Du, Q.; Cheng, K.; Yang, F. Analog synthesis of artificial humic substances for efficient removal of mercury. *Chemosphere* **2020**, *250*. [[CrossRef](#)]
28. An, Q.; Miao, Y.; Zhao, B.; Li, Z.; Zhu, S. An alkali modified biochar for enhancing Mn²⁺ adsorption: Performance and chemical mechanism. *Mater. Chem. Phys.* **2020**, *248*, 122895. [[CrossRef](#)]
29. Yi, Y.; Wang, X.; Ma, J.; Ning, P. An efficient Egeria najas-derived biochar supported nZVI composite for Cr(VI) removal: Characterisation and mechanism investigation based on Visual MINTEQ model. *Environ. Res.* **2020**, *189*, 109912. [[CrossRef](#)]
30. Zhang, H.; Xu, F.; Xue, J.; Chen, S.; Wang, J.; Yang, Y. Enhanced removal of heavy metal ions from aqueous solution using manganese dioxide-loaded biochar: Behavior and mechanism. *Sci. Rep.* **2020**, *10*, 6067. [[CrossRef](#)]
31. Wu, Z.; Chen, X.; Yuan, B.; Fu, M.L. A facile foaming-polymerisation strategy to prepare 3D MnO₂ modified biochar-based porous hydrogels for efficient removal of Cd(II) and Pb(II). *Chemosphere* **2020**, *239*. [[CrossRef](#)] [[PubMed](#)]
32. Gao, J.; Liu, Y.; Li, X.; Yang, M.; Wang, J.; Chen, Y. A promising and cost-effective biochar adsorbent derived from jujube pit for the removal of Pb(II) from aqueous solution. *Sci. Rep.* **2020**, *10*, 7473. [[CrossRef](#)]
33. Jin, Q.; Wang, Z.; Feng, Y.; Kim, Y.T.; Stewart, A.C.; O'Keefe, S.F.; Neilson, A.P.; He, Z.; Huang, H. Grape pomace and its secondary waste management: Biochar production for a broad range of lead (Pb) removal from water. *Environ. Res.* **2020**, *186*, 109442. [[CrossRef](#)] [[PubMed](#)]
34. Zhang, S.; Du, Q.; Sun, Y.; Song, J.; Yang, F.; Tsang, D.C.W. Fabrication of L-cysteine stabilised α -FeOOH nanocomposite on porous hydrophilic biochar as an effective adsorbent for Pb²⁺ removal. *Sci. Total Environ.* **2020**, *720*, 137415. [[CrossRef](#)]
35. Niu, Z.; Feng, W.; Huang, H.; Wang, B.; Chen, L.; Miao, Y.; Su, S. Green synthesis of a novel Mn–Zn ferrite/biochar composite from waste batteries and pine sawdust for Pb²⁺ removal. *Chemosphere* **2020**, *252*, 126529. [[CrossRef](#)]
36. Guo, Z.; Chen, R.; Yang, R.; Yang, F.; Chen, J.; Li, Y.; Zhou, R.; Xu, J. Synthesis of amino-functionalised biochar/spinel ferrite magnetic composites for low-cost and efficient elimination of Ni(II) from wastewater. *Sci. Total Environ.* **2020**, *722*, 137822. [[CrossRef](#)]
37. Sajjadi, B.; Chen, W.Y.; Mattern, D.L.; Hammer, N.; Dorris, A. Low-temperature acoustic-based activation of biochar for enhanced removal of heavy metals. *J. Water Process Eng.* **2020**, *34*, 101166. [[CrossRef](#)]
38. Jing, F.; Chen, C.; Chen, X.; Liu, W.; Wen, X.; Hu, S.; Yang, Z.; Guo, B.; Xu, Y.; Yu, Q. Effects of wheat straw derived biochar on cadmium availability in a paddy soil and its accumulation in rice. *Environ. Pollut.* **2020**, *257*, 113592. [[CrossRef](#)]
39. Gao, L.-Y.; Deng, J.-H.; Huang, G.-F.; Li, K.; Cai, K.-Z.; Liu, Y.; Huang, F. Relative distribution of Cd²⁺ adsorption mechanisms on biochars derived from rice straw and sewage sludge. *Bioresour. Technol.* **2019**, *272*, 114–122. [[CrossRef](#)] [[PubMed](#)]
40. Kim, W.-K.; Shim, T.; Kim, Y.-S.; Hyun, S.; Ryu, C.; Park, Y.-K.; Jung, J. Characterization of cadmium removal from aqueous solution by biochar produced from a giant Miscanthus at different pyrolytic temperatures. *Bioresour. Technol.* **2013**, *138*, 266–270. [[CrossRef](#)]
41. Usman, A.; Sallam, A.; Zhang, M.; Vithanage, M.; Ahmad, M.; Al-Farraj, A.; Ok, Y.S.; Abduljabbar, A.; Al-Wabel, M. Sorption Process of Date Palm Biochar for Aqueous Cd (II) Removal: Efficiency and Mechanisms. *WaterAir Soil Pollut.* **2016**, *227*, 449. [[CrossRef](#)]
42. Teng, D.; Zhang, B.; Xu, G.; Wang, B.; Mao, K.; Wang, J.; Sun, J.; Feng, X.; Yang, Z.; Zhang, H. Efficient removal of Cd(II) from aqueous solution by pinecone biochar: Sorption performance and governing mechanisms. *Environ. Pollut.* **2020**, *265*, 115001. [[CrossRef](#)]
43. Cheng, Q.; Huang, Q.; Khan, S.; Liu, Y.; Liao, Z.; Li, G.; Ok, Y.S. Adsorption of Cd by peanut husks and peanut husk biochar from aqueous solutions. *Ecol. Eng.* **2016**, *87*, 240–245. [[CrossRef](#)]
44. Li, B.; Yang, L.; Wang, C.; Zhang, Q.; Liu, Q.; Li, Y.; Xiao, R. Adsorption of Cd(II) from aqueous solutions by rape straw biochar derived from different modification processes. *Chemosphere* **2017**, *175*, 332–340. [[CrossRef](#)] [[PubMed](#)]
45. Akgül, G.; Maden, T.B.; Diaz, E.; Jiménez, E.M. Modification of tea biochar with Mg, Fe, Mn and Al salts for efficient sorption of PO₃-4 and Cd²⁺ from aqueous solutions. *J. Water Reuse Desalin.* **2019**, *9*, 57–66. [[CrossRef](#)]

46. Li, X.; Wang, C.; Tian, J.; Liu, J.; Chen, G. Comparison of adsorption properties for cadmium removal from aqueous solution by *Enteromorpha prolifera* biochar modified with different chemical reagents. *Environ. Res.* **2020**, *186*, 109502. [[CrossRef](#)]
47. Naeem, M.A.; Imran, M.; Amjad, M.; Abbas, G.; Tahir, M.; Murtaza, B.; Zakir, A.; Shahid, M.; Bulgariu, L.; Ahmad, I. Batch and column scale removal of cadmium from water using raw and acid activated wheat straw biochar. *Water* **2019**, *11*, 1438. [[CrossRef](#)]
48. Qian, L.; Shang, X.; Zhang, B.; Zhang, W.; Su, A.; Chen, Y.; Ouyang, D.; Han, L.; Yan, J.; Chen, M. Enhanced removal of Cr(VI) by silicon rich biochar-supported nanoscale zero-valent iron. *Chemosphere* **2019**, *215*, 739–745. [[CrossRef](#)]
49. Li, H.; Dong, X.; da Silva, E.B.; de Oliveira, L.M.; Chen, Y.; Ma, L.Q. Mechanisms of metal sorption by biochars: Biochar characteristics and modifications. *Chemosphere* **2017**, *178*, 466–478. [[CrossRef](#)]
50. Qu, J.; Meng, X.; Zhang, Y.; Meng, Q.; Tao, Y.; Hu, Q.; Jiang, X.; You, H.; Shoemaker, C.A. A combined system of microwave-functionalised rice husk and poly-aluminium chloride for trace cadmium-contaminated source water purification: Exploration of removal efficiency and mechanism. *J. Hazard. Mater.* **2019**, *379*, 120804. [[CrossRef](#)] [[PubMed](#)]
51. Dong, X.; Ma, L.Q.; Zhu, Y.; Li, Y.; Gu, B. Mechanistic Investigation of Mercury Sorption by Brazilian Pepper Biochars of Different Pyrolytic Temperatures Based on X-ray Photoelectron Spectroscopy and Flow Calorimetry. *Environ. Sci. Technol.* **2013**, *47*, 12156–12164. [[CrossRef](#)]
52. Shen, Y.-S.; Wang, S.-L.; Tzou, Y.-M.; Yan, Y.-Y.; Kuan, W.-H. Removal of hexavalent Cr by coconut coir and derived chars—The effect of surface functionality. *Bioresour. Technol.* **2012**, *104*, 165–172. [[CrossRef](#)]
53. Li, F.; Zimmerman, A.R.; Hu, X.; Gao, B. Removal of aqueous Cr(VI) by Zn- and Al-modified hydrochar. *Chemosphere* **2020**, *260*, 127610. [[CrossRef](#)]
54. Sun, Y.; Yu, I.K.M.; Tsang, D.C.W.; Cao, X.; Lin, D.; Wang, L.; Graham, N.J.D.; Alessi, D.S.; Komárek, M.; Ok, Y.S.; et al. Multifunctional iron-biochar composites for the removal of potentially toxic elements, inherent cations, and hetero-chloride from hydraulic fracturing wastewater. *Environ. Int.* **2019**, *124*, 521–532. [[CrossRef](#)] [[PubMed](#)]
55. Qu, J.; Wang, Y.; Tian, X.; Jiang, Z.; Deng, F.; Tao, Y.; Jiang, Q.; Wang, L.; Zhang, Y. KOH-activated porous biochar with high specific surface area for adsorptive removal of chromium (VI) and naphthalene from water: Affecting factors, mechanisms and reusability exploration. *J. Hazard. Mater.* **2021**, *401*, 123292. [[CrossRef](#)]
56. Xu, X.; Schierz, A.; Xu, N.; Cao, X. Comparison of the characteristics and mechanisms of Hg(II) sorption by biochars and activated carbon. *J. Colloid Interface Sci.* **2016**, *463*, 55–60. [[CrossRef](#)] [[PubMed](#)]
57. Liu, P.; Ptacek, C.J.; Blowes, D.W.; Landis, R.C. Mechanisms of mercury removal by biochars produced from different feedstocks determined using X-ray absorption spectroscopy. *J. Hazard. Mater.* **2016**, *308*, 233–242. [[CrossRef](#)]
58. Liu, P.; Ptacek, C.J.; Elena, K.M.A.; Blowes, D.W.; Gould, W.D.; Finfrock, Y.Z.; Wang, A.O.; Landis, R.C. Evaluation of mercury stabilisation mechanisms by sulfurised biochars determined using X-ray absorption spectroscopy. *J. Hazard. Mater.* **2018**, *347*, 114–122. [[CrossRef](#)] [[PubMed](#)]
59. Wang, J.; Wang, J.; Zhang, Y.; Wang, T.; Pan, W.-P. Ionic mercury captured by H₂S sulfurised biochar in liquid hydrocarbons: Mechanism and stability evaluation. *Fuel* **2020**, *278*, 118413. [[CrossRef](#)]
60. Feng, Y.; Liu, P.; Wang, Y.; Liu, W.; Liu, Y.Y.; Finfrock, Y.Z. Mechanistic investigation of mercury removal by unmodified and Fe-modified biochars based on synchrotron-based methods. *Sci. Total Environ.* **2020**, *719*, 137435. [[CrossRef](#)]
61. Shan, Y.; Yang, W.; Li, Y.; Liu, Y.; Pan, J. Preparation of microwave-activated magnetic bio-char adsorbent and study on removal of elemental mercury from flue gas. *Sci. Total Environ.* **2019**, *697*, 134049. [[CrossRef](#)]
62. Yu, W.; Lian, F.; Cui, G.; Liu, Z. N-doping effectively enhances the adsorption capacity of biochar for heavy metal ions from aqueous solution. *Chemosphere* **2018**, *193*, 8–16. [[CrossRef](#)]
63. Lee, M.-E.; Park, J.H.; Chung, J.W. Comparison of the lead and copper adsorption capacities of plant source materials and their biochars. *J. Environ. Manag.* **2019**, *236*, 118–124. [[CrossRef](#)]
64. Shen, Z.; Hou, D.; Jin, F.; Shi, J.; Fan, X.; Tsang, D.C.W.; Alessi, D.S. Effect of production temperature on lead removal mechanisms by rice straw biochars. *Sci. Total Environ.* **2019**, *655*, 751–758. [[CrossRef](#)]
65. Zama, E.F.; Zhu, Y.-G.; Reid, B.J.; Sun, G.-X. The role of biochar properties in influencing the sorption and desorption of Pb(II), Cd(II) and As(III) in aqueous solution. *J. Clean. Prod.* **2017**, *148*, 127–136. [[CrossRef](#)]

66. Ding, Z.; Hu, X.; Wan, Y.; Wang, S.; Gao, B. Removal of lead, copper, cadmium, zinc, and nickel from aqueous solutions by alkali-modified biochar: Batch and column tests. *J. Ind. Eng. Chem.* **2016**, *33*, 239–245. [[CrossRef](#)]
67. Wu, W.; Li, J.; Lan, T.; Müller, K.; Niazi, N.K.; Chen, X.; Xu, S.; Zheng, L.; Chu, Y.; Li, J.; et al. Unraveling sorption of lead in aqueous solutions by chemically modified biochar derived from coconut fiber: A microscopic and spectroscopic investigation. *Sci. Total Environ.* **2017**, *576*, 766–774. [[CrossRef](#)]
68. Wang, S.; Gao, B.; Li, Y.; Mosa, A.; Zimmerman, A.R.; Ma, L.Q.; Harris, W.G.; Migliaccio, K.W. Manganese oxide-modified biochars: Preparation, characterisation, and sorption of arsenate and lead. *Bioresour. Technol.* **2015**, *181*, 13–17. [[CrossRef](#)]
69. Deng, J.; Liu, Y.; Liu, S.; Zeng, G.; Tan, X.; Huang, B.; Tang, X.; Wang, S.; Hua, Q.; Yan, Z. Competitive adsorption of Pb(II), Cd(II) and Cu(II) onto chitosan-pyromellitic dianhydride modified biochar. *J. Colloid Interface Sci.* **2017**, *506*, 355–364. [[CrossRef](#)]
70. Iftthikar, J.; Jiao, X.; Ngambia, A.; Wang, T.; Khan, A.; Jawad, A.; Xue, Q.; Liu, L.; Chen, Z. Facile One-Pot Synthesis of Sustainable Carboxymethyl Chitosan—Sewage Sludge Biochar for Effective Heavy Metal Chelation and Regeneration. *Bioresour. Technol.* **2018**, *262*, 22–31. [[CrossRef](#)]
71. Bartolomeu, M.; Neves, M.G.P.M.S.; Faustino, M.A.F.; Almeida, A. Wastewater chemical contaminants: Remediation by advanced oxidation processes. *Photochem. Photobiol. Sci.* **2018**, *17*, 1573–1598. [[CrossRef](#)]
72. D’Alessio, M.; Onanong, S.; Snow, D.D.; Ray, C. Occurrence and removal of pharmaceutical compounds and steroids at four wastewater treatment plants in Hawai’i and their environmental fate. *Sci. Total Environ.* **2018**, *631–632*, 1360–1370. [[CrossRef](#)]
73. Nantaba, F.; Wasswa, J.; Kylin, H.; Palm, W.U.; Bouwman, H.; Kümmerer, K. Occurrence, distribution, and ecotoxicological risk assessment of selected pharmaceutical compounds in water from Lake Victoria, Uganda. *Chemosphere* **2020**, *239*, 124642. [[CrossRef](#)]
74. Ebele, A.J.; Oluseyi, T.; Drage, D.S.; Harrad, S.; Abou-Elwafa Abdallah, M. Occurrence, seasonal variation and human exposure to pharmaceuticals and personal care products in surface water, groundwater and drinking water in Lagos State, Nigeria. *Emerg. Contam.* **2020**, *6*, 124–132. [[CrossRef](#)]
75. Hansen, S.P.; Messer, T.L.; Mittelstet, A.R. Mitigating the risk of atrazine exposure: Identifying hot spots and hot times in surface waters across Nebraska, USA. *J. Environ. Manag.* **2019**, *250*, 109424. [[CrossRef](#)] [[PubMed](#)]
76. Vacchi, F.I.; de Souza Vendemiatti, J.A.; da Silva, B.F.; Zanoni, M.V.B.; de Aragão Umbuzeiro, G. Quantifying the contribution of dyes to the mutagenicity of waters under the influence of textile activities. *Sci. Total Environ.* **2017**, *601–602*, 230–236. [[CrossRef](#)]
77. Hernández-Abreu, A.B.; Álvarez-Torrellas, S.; Águeda, V.I.; Larriba, M.; Delgado, J.A.; Calvo, P.A.; García, J. Enhanced removal of the endocrine disruptor compound Bisphenol A by adsorption onto green-carbon materials. Effect of real effluents on the adsorption process. *J. Environ. Manag.* **2020**, *266*. [[CrossRef](#)]
78. Tran, H.N.; Tomul, F.; Thi Hoang Ha, N.; Nguyen, D.T.; Lima, E.C.; Le, G.T.; Chang, C.T.; Masindi, V.; Woo, S.H. Innovative spherical biochar for pharmaceutical removal from water: Insight into adsorption mechanism. *J. Hazard. Mater.* **2020**, *394*, 122255. [[CrossRef](#)]
79. Zhang, R.; Li, Y.; Wang, Z.; Tong, Y.; Sun, P. Biochar-activated peroxydisulfate as an effective process to eliminate pharmaceutical and metabolite in hydrolysed urine. *Water Res.* **2020**, *177*, 115809. [[CrossRef](#)]
80. Deng, R.; Luo, H.; Huang, D.; Zhang, C. Biochar-mediated Fenton-like reaction for the degradation of sulfamethazine: Role of environmentally persistent free radicals. *Chemosphere* **2020**, *255*, 126975. [[CrossRef](#)]
81. Cheng, D.; Ngo, H.H.; Guo, W.; Chang, S.W.; Nguyen, D.D.; Zhang, X.; Varjani, S.; Liu, Y. Feasibility study on a new pomelo peel derived biochar for tetracycline antibiotics removal in swine wastewater. *Sci. Total Environ.* **2020**, *720*, 137662. [[CrossRef](#)]
82. Kim, J.E.; Bhatia, S.K.; Song, H.J.; Yoo, E.; Jeon, H.J.; Yoon, J.Y.; Yang, Y.; Gurav, R.; Yang, Y.H.; Kim, H.J.; et al. Adsorptive removal of tetracycline from aqueous solution by maple leaf-derived biochar. *Bioresour. Technol.* **2020**, *306*, 123092. [[CrossRef](#)]
83. Xiang, W.; Wan, Y.; Zhang, X.; Tan, Z.; Xia, T.; Zheng, Y.; Gao, B. Adsorption of tetracycline hydrochloride onto ball-milled biochar: Governing factors and mechanisms. *Chemosphere* **2020**, *255*, 127057. [[CrossRef](#)]
84. Zhang, H.; Lu, T.; Wang, M.; Jin, R.; Song, Y.; Zhou, Y.; Qi, Z.; Chen, W. Inhibitory role of citric acid in the adsorption of tetracycline onto biochars: Effects of solution pH and Cu²⁺. *Colloids Surf. A Physicochem. Eng. Asp.* **2020**, *595*. [[CrossRef](#)]
85. Dai, J.; Meng, X.; Zhang, Y.; Huang, Y. Effects of modification and magnetisation of rice straw derived biochar on adsorption of tetracycline from water. *Bioresour. Technol.* **2020**, *311*, 123455. [[CrossRef](#)]

86. Qiu, Y.; Xu, X.; Xu, Z.; Liang, J.; Yu, Y.; Cao, X. Contribution of different iron species in the iron-biochar composites to sorption and degradation of two dyes with varying properties. *Chem. Eng. J.* **2020**, *389*, 124471. [[CrossRef](#)]
87. Zubair, M.; Manzar, M.S.; Mu'azu, N.D.; Anil, I.; Blaisi, N.I.; Al-Harathi, M.A. Functionalized MgAl-layered hydroxide intercalated date-palm biochar for Enhanced Uptake of Cationic dye: Kinetics, isotherm and thermodynamic studies. *Appl. Clay Sci.* **2020**, *190*, 105587. [[CrossRef](#)]
88. Li, F.; Duan, F.; Ji, W.; Gui, X. Biochar-activated persulfate for organic contaminants removal: Efficiency, mechanisms and influencing factors. *Ecotoxicol. Environ. Saf.* **2020**, *198*, 110653. [[CrossRef](#)] [[PubMed](#)]
89. Yek, P.N.Y.; Peng, W.; Wong, C.C.; Liew, R.K.; Ho, Y.L.; Wan Mahari, W.A.; Azwar, E.; Yuan, T.Q.; Tabatabaei, M.; Aghbashlo, M.; et al. Engineered biochar via microwave CO₂ and steam pyrolysis to treat carcinogenic Congo red dye. *J. Hazard. Mater.* **2020**, *395*. [[CrossRef](#)]
90. Keerthanan, S.; Bhatnagar, A.; Mahatantila, K.; Jayasinghe, C.; Ok, Y.S.; Vithanage, M. Engineered tea-waste biochar for the removal of caffeine, a model compound in pharmaceuticals and personal care products (PPCPs), from aqueous media. *Environ. Technol. Innov.* **2020**, *19*, 100847. [[CrossRef](#)]
91. Yang, J.; Pan, B.; Li, H.; Liao, S.; Zhang, D.; Wu, M.; Xing, B. Degradation of p-Nitrophenol on Biochars: Role of Persistent Free Radicals. *Environ. Sci. Technol.* **2016**, *50*, 694–700. [[CrossRef](#)]
92. Abdul, G.; Zhu, X.; Chen, B. Structural characteristics of biochar-graphene nanosheet composites and their adsorption performance for phthalic acid esters. *Chem. Eng. J.* **2017**, *319*, 9–20. [[CrossRef](#)]
93. Zhang, X.N.; Mao, G.Y.; Jiao, Y.B.; Shang, Y.; Han, R.P. Adsorption of anionic dye on magnesium hydroxide-coated pyrolytic bio-char and reuse by microwave irradiation. *Int. J. Environ. Sci. Technol.* **2014**, *11*, 1439–1448. [[CrossRef](#)]
94. Acevedo-García, V.; Rosales, E.; Puga, A.; Pazos, M.; Sanromán, M.A. Synthesis and use of efficient adsorbents under the principles of circular economy: Waste valorisation and electroadvanced oxidation process regeneration. *Sep. Purif. Technol.* **2020**, *242*, 116796. [[CrossRef](#)]
95. Reguyal, F.; Sarmah, A.K.; Gao, W. Synthesis of magnetic biochar from pine sawdust via oxidative hydrolysis of FeCl₂ for the removal sulfamethoxazole from aqueous solution. *J. Hazard. Mater.* **2017**, *321*, 868–878. [[CrossRef](#)]
96. Puga, A.; Rosales, E.; Pazos, M.; Sanromán, M.A. Prompt removal of antibiotic by adsorption/electro-Fenton degradation using an iron-doped perlite as heterogeneous catalyst. *Process Saf. Environ. Prot.* **2020**, *144*, 100–110. [[CrossRef](#)]
97. Chen, Y.; Lin, Y.-C.; Ho, S.-H.; Zhou, Y.; Ren, N. Highly efficient adsorption of dyes by biochar derived from pigments-extracted macroalgae pyrolysed at different temperature. *Bioresour. Technol.* **2018**, *259*, 104–110. [[CrossRef](#)] [[PubMed](#)]
98. Dai, L.; Zhu, W.; He, L.; Tan, F.; Zhu, N.; Zhou, Q.; He, M.; Hu, G. Calcium-rich biochar from crab shell: An unexpected super adsorbent for dye removal. *Bioresour. Technol.* **2018**, *267*, 510–516. [[CrossRef](#)]
99. Peterson, S.C.; Jackson, M.A.; Kim, S.; Palmquist, D.E. Increasing biochar surface area: Optimisation of ball milling parameters. *Powder Technol.* **2012**, *228*, 115–120. [[CrossRef](#)]
100. Lyu, H.; Gao, B.; He, F.; Zimmerman, A.R.; Ding, C.; Tang, J.; Crittenden, J.C. Experimental and modeling investigations of ball-milled biochar for the removal of aqueous methylene blue. *Chem. Eng. J.* **2018**, *335*, 110–119. [[CrossRef](#)]
101. Inyang, M.I.; Gao, B.; Yao, Y.; Xue, Y.; Zimmerman, A.; Mosa, A.; Pullammanappallil, P.; Ok, Y.S.; Cao, X. A review of biochar as a low-cost adsorbent for aqueous heavy metal removal. *Crit. Rev. Environ. Sci. Technol.* **2016**, *46*, 406–433. [[CrossRef](#)]
102. Rajapaksha, A.U.; Chen, S.S.; Tsang, D.C.W.; Zhang, M.; Vithanage, M.; Mandal, S.; Gao, B.; Bolan, N.S.; Ok, Y.S. Engineered/designer biochar for contaminant removal/immobilisation from soil and water: Potential and implication of biochar modification. *Chemosphere* **2016**, *148*, 276–291. [[CrossRef](#)] [[PubMed](#)]
103. Qian, W.-C.; Luo, X.-P.; Wang, X.; Guo, M.; Li, B. Removal of methylene blue from aqueous solution by modified bamboo hydrochar. *Ecotoxicol. Environ. Saf.* **2018**, *157*, 300–306. [[CrossRef](#)] [[PubMed](#)]
104. Wang, L.; Yan, W.; He, C.; Wen, H.; Cai, Z.; Wang, Z.; Chen, Z.; Liu, W. Microwave-assisted preparation of nitrogen-doped biochars by ammonium acetate activation for adsorption of acid red 18. *Appl. Surf. Sci.* **2018**, *433*, 222–231. [[CrossRef](#)]

105. Xu, X.; Zheng, Y.; Gao, B.; Cao, X. N-doped biochar synthesised by a facile ball-milling method for enhanced sorption of CO₂ and reactive red. *Chem. Eng. J.* **2019**, *368*, 564–572. [[CrossRef](#)]
106. Meili, L.; Lins, P.V.; Zanta, C.L.P.S.; Soletti, J.I.; Ribeiro, L.M.O.; Dornelas, C.B.; Silva, T.L.; Vieira, M.G.A. MgAl-LDH/Biochar composites for methylene blue removal by adsorption. *Appl. Clay Sci.* **2019**, *168*, 11–20. [[CrossRef](#)]
107. Zhang, P.; O'Connor, D.; Wang, Y.; Jiang, L.; Xia, T.; Wang, L.; Tsang, D.C.W.; Ok, Y.S.; Hou, D. A green biochar/iron oxide composite for methylene blue removal. *J. Hazard. Mater.* **2020**, *384*, 121286. [[CrossRef](#)]
108. Du, C.; Song, Y.; Shi, S.; Jiang, B.; Yang, J.; Xiao, S. Preparation and characterisation of a novel Fe₃O₄-graphene-biochar composite for crystal violet adsorption. *Sci. Total Environ.* **2020**, *711*, 134662. [[CrossRef](#)]
109. Zeng, Z.; Ye, S.; Wu, H.; Xiao, R.; Zeng, G.; Liang, J.; Zhang, C.; Yu, J.; Fang, Y.; Song, B. Research on the sustainable efficacy of g-MoS₂ decorated biochar nanocomposites for removing tetracycline hydrochloride from antibiotic-polluted aqueous solution. *Sci. Total Environ.* **2019**, *648*, 206–217. [[CrossRef](#)] [[PubMed](#)]
110. Xiong, X.; Yu, I.K.M.; Cao, L.; Tsang, D.C.W.; Zhang, S.; Ok, Y.S. A review of biochar-based catalysts for chemical synthesis, biofuel production, and pollution control. *Bioresour. Technol.* **2017**, *246*, 254–270. [[CrossRef](#)] [[PubMed](#)]
111. Cho, D.-W.; Yoon, K.; Ahn, Y.; Sun, Y.; Tsang, D.C.W.; Hou, D.; Ok, Y.S.; Song, H. Fabrication and environmental applications of multifunctional mixed metal-biochar composites (MMBC) from red mud and lignin wastes. *J. Hazard. Mater.* **2019**, *374*, 412–419. [[CrossRef](#)]
112. Heo, J.; Yoon, Y.; Lee, G.; Kim, Y.; Han, J.; Park, C.M. Enhanced adsorption of bisphenol A and sulfamethoxazole by a novel magnetic CuZnFe₂O₄-biochar composite. *Bioresour. Technol.* **2019**, *281*, 179–187. [[CrossRef](#)]
113. Solanki, A.; Boyer, T.H. Pharmaceutical removal in synthetic human urine using biochar. *Environ. Sci. Water Res. Technol.* **2017**, *3*, 553–565. [[CrossRef](#)]
114. Chakraborty, P.; Show, S.; Banerjee, S.; Halder, G. Mechanistic insight into sorptive elimination of ibuprofen employing bi-directional activated biochar from sugarcane bagasse: Performance evaluation and cost estimation. *J. Environ. Chem. Eng.* **2018**, *6*, 5287–5300. [[CrossRef](#)]
115. Yang, Y.Q.; Cui, M.H.; Ren, Y.G.; Guo, J.C.; Zheng, Z.Y.; Liu, H. Towards Understanding the Mechanism of Heavy Metals Immobilization in Biochar Derived from Co-pyrolysis of Sawdust and Sewage Sludge. *Bull. Environ. Contam. Toxicol.* **2020**, *104*, 489–496. [[CrossRef](#)]
116. Shen, T.; Tang, Y.; Lu, X.Y.; Meng, Z. Mechanisms of copper stabilisation by mineral constituents in sewage sludge biochar. *J. Clean. Prod.* **2018**, *193*, 185–193. [[CrossRef](#)]
117. Huang, H.J.; Yang, T.; Lai, F.Y.; Wu, G.Q. Co-pyrolysis of sewage sludge and sawdust/rice straw for the production of biochar. *J. Anal. Appl. Pyrolysis* **2017**, *125*, 61–68. [[CrossRef](#)]
118. Meng, J.; Liang, S.; Tao, M.; Liu, X.; Brookes, P.C.; Xu, J. Chemical speciation and risk assessment of Cu and Zn in biochars derived from co-pyrolysis of pig manure with rice straw. *Chemosphere* **2018**, *200*, 344–350. [[CrossRef](#)]
119. Liu, L.; Huang, L.; Huang, R.; Lin, H.; Wang, D. Immobilization of heavy metals in biochar derived from co-pyrolysis of sewage sludge and calcium sulfate. *J. Hazard. Mater.* **2021**, *403*. [[CrossRef](#)] [[PubMed](#)]
120. Jin, J.; Wang, M.; Cao, Y.; Wu, S.; Liang, P.; Li, Y.; Zhang, J.; Zhang, J.; Wong, M.H.; Shan, S.; et al. Cumulative effects of bamboo sawdust addition on pyrolysis of sewage sludge: Biochar properties and environmental risk from metals. *Bioresour. Technol.* **2017**, *228*, 218–226. [[CrossRef](#)]
121. Ndirangu, S.M.; Liu, Y.; Xu, K.; Song, S. Risk Evaluation of Pyrolyzed Biochar from Multiple Wastes. *J. Chem.* **2019**, *2019*. [[CrossRef](#)]
122. Rosales, E.; Ferreira, L.; Sanromán, M.Á.; Tavares, T.; Pazos, M. Enhanced selective metal adsorption on optimised agroforestry waste mixtures. *Bioresour. Technol.* **2015**, *182*, 41–49. [[CrossRef](#)]
123. Dai, Y.; Zhang, N.; Xing, C.; Cui, Q.; Sun, Q. The adsorption, regeneration and engineering applications of biochar for removal organic pollutants: A review. *Chemosphere* **2019**, *223*, 12–27. [[CrossRef](#)]
124. Hassan, M.; Naidu, R.; Du, J.; Liu, Y.; Qi, F. Critical review of magnetic biosorbents: Their preparation, application, and regeneration for wastewater treatment. *Sci. Total Environ.* **2020**, *702*, 134893. [[CrossRef](#)] [[PubMed](#)]
125. He, R.; Peng, Z.; Lyu, H.; Huang, H.; Nan, Q.; Tang, J. Synthesis and characterisation of an iron-impregnated biochar for aqueous arsenic removal. *Sci. Total Environ.* **2018**, *612*, 1177–1186. [[CrossRef](#)]

126. Gupta, V.K.; Nayak, A. Cadmium removal and recovery from aqueous solutions by novel adsorbents prepared from orange peel and Fe₂O₃ nanoparticles. *Chem. Eng. J.* **2012**, *180*, 81–90. [[CrossRef](#)]
127. Qiao, K.; Tian, W.; Bai, J.; Dong, J.; Zhao, J.; Gong, X.; Liu, S. Preparation of biochar from *Enteromorpha prolifera* and its use for the removal of polycyclic aromatic hydrocarbons (PAHs) from aqueous solution. *Ecotoxicol. Environ. Saf.* **2018**, *149*, 80–87. [[CrossRef](#)] [[PubMed](#)]
128. Lartey-Young, G.; Ma, L. Remediation with Semicoke-Preparation, Characterisation, and Adsorption Application. *Materials* **2020**, *13*, 4334. [[CrossRef](#)]
129. Yu, F.; Wang, L.; Ma, H.; Pan, Y. Zeolitic imidazolate framework-8 modified active carbon fiber as an efficient cathode in electro-Fenton for tetracycline degradation. *Sep. Purif. Technol.* **2020**, *237*, 116342. [[CrossRef](#)]
130. Fdez-Sanromán, A.; Acevedo-García, V.; Pazos, M.; Sanromán, M.Á.; Rosales, E. Iron-doped cathodes for electro-Fenton implementation: Application for pymetrozine degradation. *Electrochim. Acta* **2020**, *338*, 135768. [[CrossRef](#)]
131. Li, X.; Jia, Y.; Zhou, M.; Su, X.; Sun, J. High-efficiency degradation of organic pollutants with Fe, N co-doped biochar catalysts via persulfate activation. *J. Hazard. Mater.* **2020**, *397*, 122764. [[CrossRef](#)]
132. Mer, K.; Sajjadi, B.; Egiebor, N.O.; Chen, W.-Y.; Mattern, D.L.; Tao, W. Enhanced degradation of organic contaminants using catalytic activity of carbonaceous structures: A strategy for the reuse of exhausted sorbents. *J. Environ. Sci.* **2021**, *99*, 267–273. [[CrossRef](#)]
133. Zhang, H.; Tang, L.; Wang, J.; Yu, J.; Feng, H.; Lu, Y.; Chen, Y.; Liu, Y.; Wang, J.; Xie, Q. Enhanced surface activation process of persulfate by modified bagasse biochar for degradation of phenol in water and soil: Active sites and electron transfer mechanism. *Colloids Surf. A Physicochem. Eng. Asp.* **2020**, *599*, 124904. [[CrossRef](#)]
134. Lykoudi, A.; Frontistis, Z.; Vakros, J.; Manariotis, I.D.; Mantzavinos, D. Degradation of sulfamethoxazole with persulfate using spent coffee grounds biochar as activator. *J. Environ. Manag.* **2020**, *271*, 111022. [[CrossRef](#)]
135. Grand View Research. *Biochar Market Size, Share & Trends Analysis Report By Technology (Gasification, Pyrolysis), By Application (Agriculture (Farming, Livestock)), By Region, And Segment Forecasts, 2019–2025*; April 2019 San Francisco US Grand View Research Report ID: 978-1-68038-681-3; Grand View Research: San Francisco, CA, USA, 2019.
136. Krasucka, P.; Pan, B.; Sik Ok, Y.; Mohan, D.; Sarkar, B.; Oleszczuk, P. Engineered biochar—A sustainable solution for the removal of antibiotics from water. *Chem. Eng. J.* **2021**, *405*, 126926. [[CrossRef](#)]
137. Ahmed, M.B.; Zhou, J.L.; Ngo, H.N.; Guo, W. Insight into biochar properties and its cost analysis. *Biomass Bioenergy* **2016**, *84*, 76–86. [[CrossRef](#)]
138. Homagain, K.; Shahi, C.; Luckai, N.; Sharma, M. Life cycle cost and economic assessment of biochar-based bioenergy production and biochar land application in Northwestern Ontario, Canada. *For. Ecosyst.* **2016**, *3*, 21. [[CrossRef](#)]
139. Keske, C.; Godfrey, T.; Hoag, D.L.K.; Abedin, J. Economic feasibility of biochar and agriculture coproduction from Canadian black spruce forest. *Food Energy Secur.* **2020**, *9*, e188. [[CrossRef](#)]

Publisher's Note: MDPI stays neutral with regard to jurisdictional claims in published maps and institutional affiliations.



© 2020 by the authors. Licensee MDPI, Basel, Switzerland. This article is an open access article distributed under the terms and conditions of the Creative Commons Attribution (CC BY) license (<http://creativecommons.org/licenses/by/4.0/>).